Available online at www.CivileJournal.org

Civil Engineering Journal

(E-ISSN: 2476-3055; ISSN: 2676-6957)

Vol. 9, No. 04, April, 2023

Experimental Establishing of Moving Hydraulic Jump in a Trapezoidal Channel

Najah K. Al-Bedyry [1], Maher A. A. Kadim [2], Saman H. Hussein [3], Zainab S. Al-Khafaji [4, 5*], Fatimah N. Al-Husseinawi [6]

[1] *Department of Civil Engineering, College of Engineering, University of Babylon, Babylon, Iraq.*

[2] *Department of Building and Construction Technical, Al-Mussaib Technical College, Al-Furat Al-Awsat Technical University, Babylon, Iraq.*

[3] *Department of Civil Engineering, College of Engineering, University of Sulaimani, Sulaimani, Iraq.*

[4] *Department of Civil Engineering, Universiti Kebangsaan Malaysia, 43600 Bangi, Selangor, Malaysia.*

[5] *Department of Building and Construction Techniques Engineering, Al-Mustaqbal University College, 51001 Hillah, Babylon, Iraq.*

[6] *Department of Civil Engineering, Liverpool John Moores University, Liverpool, L3 3AF, United Kingdom.*

Received 03 December 2022; Revised 11 March 2023; Accepted 17 March 2023; Published 01 April 2023

Abstract

This research was prepared as a preliminary laboratory study to achieve a moving hydraulic jump with controlled discharges. It is an initial part of the study that is being prepared to treat the salt tide occurring in the Shatt al-Arab due to the lack of water imports that were coming from the Karun and Karkheh rivers from Iranian territory, as this scarcity caused a salt tide that affected significantly the environmental reality of the city of Basra and the agricultural lands surrounding the Shatt al-Arab, such as the Shatt al-Arab district and the Siba orchards. As part of the proposed solutions, a moving hydraulic jump is created that pushes the salt tongue into the Persian Gulf; the results were promising. A moving hydraulic leap is a good example of unstable super- and sub-critical flow regimes and is regarded as a specific case of unsteady flow in a channel. There aren't many published experiments on this particular flow type, and the quantitative simulation of such a flow state has some inherent complexity. An experimental setup was created for this work in order to assess the hydraulic performance of a moving hydraulic jump in a trapezoidal flume. A sluice gate was installed at the flume's upstream edge to provide an unstable supercritical flow regime, movable hydraulic jumps along the channel, and temporal water stages at the gate's upstream side for the various downstream end boundary situations. Several flow factors, including energy head, pressure head, and flow depth, were estimated from the recorded data. The study found connections between discharge and shifting hydraulic jump variables. By employing relatively stable momentum and energy formulas, simple and time-independent formulas were developed that accurately predicted the pressure head in the subcritical region of an unstable mixed flow. As a result, the moving hydraulic jump factor can be correctly predicted using time-independent correlations by using the discharge variation as a boundary scenario.

Keywords: Subcritical; Supercritical; Hydraulic Jump; Temporal Water Stages.

1. Introduction

In a variety of disciplines, including water resources and hydraulic engineering, numerical simulations were widely used for investigating flow behavior and forecasting flow situations due to their numerous obvious benefits, although there were numerous problems of considerable concern that these effective tools did not fully address [1–3]. Physical models offer straightforward and useful solutions in these situations. Similarly, they offer trustworthy data that may be

* Corresponding author: p123005@siswa.ukm.edu.my

http://dx.doi.org/10.28991/CEJ-2023-09-04-08

utilized to validate numerical models in conjunction with field measurements [4–6]. Numerous numerical methods have been introduced thus far for studying mixed convection in cross-flow systems. Any flow scenarios that can arise in real-world settings should be able to be handled by these procedures [7–9].

The moving hydraulic jump, where the flow regimes of supercritical and subcritical vary, is one of the well-known situations that still needs additional research and analysis. Therefore, having access to enough data on how this type of flow behaves under various situations will help us comprehend the phenomena and enable us to create solid numerical schemes or, at the very least, enhance our current ones. Moving hydraulic jumps frequently occur in real-world settings. Control gates, weirs, and culverts are a few hydraulic structures in an irrigation network that can produce, assimilate, or transfer movement hydraulically during proper usage or over a certain release range [10–13]. Figure 1, for example, shows a collection of control structures that create this flow type in a channel. In this circumstance, it is customary to modify the outflow at the channel head or in the auxiliary offtakes according to the water supply schedule, which alters the surface of the water pattern and moves the trans-flow rate forward. Moreover, natural streams are the most likely places for moving hydraulic jumps throughout a flood event, particularly when blocking buildings like bridges are positioned along the channel [14–16]. Modifications to the longitudinal profile of the channel or variations in boundary roughness may also cause the occurrence of unstable mixed flow regimes. Following a dam failure, a channel reach frequently exhibits coexisting subcritical and supercritical flow. This instance effectively illustrates the prevalence of varied flow conditions, their relevance to realistic applications, and the need for additional study to gain the knowledge necessary to manage them [17–18]. Bijankhan & Kouchakzadeh [19] studied the flow through parallel sluice gates under low flow delivery conditions. They experimentally indicated that the stage-discharge curve is affected when some gates are closed. Based on the incomplete self-similarity method, they presented a new stage-discharge relationship for parallel sluice gates under low-flow delivery conditions. More recently, Shaddehi & Bijankhan [20] indicated experimentally that the downstream measuring location affects the accuracy of the relationship of the conjugated depth. Sauida [21] studied a wide range of flow conditions downstream of parallel gates, observed the reverse and forward flows, and concluded that a separation plane exists between these two flows. Furthermore, using experimental data, Sauida proposed a multi-regression relationship for determining the discharge coefficient for parallel gates.

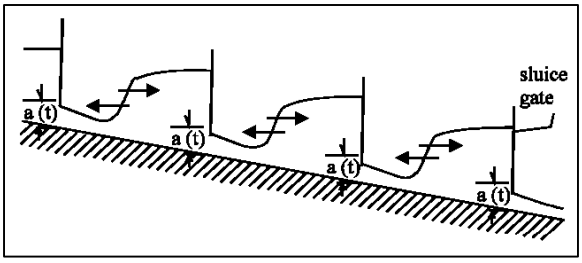

Figure 1. Successive sluice gate closures in a stream flume

The main characteristic of hybrid flow patterns, to which particular attention should still be compensated while simulating this type of flow, is the varied orientations in which waves propagate in sub- and super-critical flows. When simulating such flow scenarios, an adequate numerical solution should always be able to convey shock and flow discontinuity, account for the direction in which waves propagate, and consider suitable boundary situations for each flow regime [22]. The systems of governing formulas for aerodynamics have been solved utilizing various finite variance shock-capturing approaches. There have been attempts to use such methods to solve the Saint-Venant formulas and capture the shock due to the similarities between small-depth water formulas and the hydraulic equation for compliant flow. Although the numerical approach is commonly considered a criterion for resolving a single open flow pattern and is appropriate for subcritical and supercritical flow regimes, mixed flow conditions cannot be resolved using this approach.

In contrast to the mathematical challenges brought on by the existence of both sub- and supercritical flows, the practical examinations of these flows also call for specialized laboratory procedures to gather the necessary temporal data. The one-dimensional flow-controlling formulas can describe fluids, including hydraulic discontinuities and jumps. The following is typically how these formulas' conservation form is stated for horizontal channels with little friction:

$$\frac{\partial u}{\partial t} + \mathrm{K}\frac{\partial u}{\partial x} = 0 \quad (1)$$

Where as $u \propto [A, Q]$, A is cross-sectional flow area, Q is discharge, V is mean velocity, and K is a fixed constant. Ratio of Flow Velocity to Wave Speed (c): Froude number $Fr = \frac{V}{c}$, and $c = \sqrt{\frac{gA}{b}}$ where: c is wave speed, b = width of the channel at the flow surface, and (g) is gravitational acceleration.

Once an interruption and flow state variables are discovered in a discharge situation, it is impossible to explain the flow scenario using a different version of the guiding formula [23]. However, it is possible to use the integral form of these formulas if a discontinuity manifests in the feasible region. Nevertheless, many commercial flood routing models

could not provide a satisfactory solution due to some numerical issues [24]. It is very challenging to collect the necessary information for this type of release [25]. Hence, it is crucial to gather pertinent and trustworthy data utilizing experimental settings to explore this phenomenon and test and validate numerical simulations [26, 27]. Nevertheless, it was noted that the availability of such data was extremely limited and had drawbacks. Therefore, efforts in this direction will further knowledge of the phenomenon and appear necessary [24]. In this study, moving hydraulic leaps, examples of unsteady mixed flow regimes, were studied using an experimental system. Data analysis showed that there were precise correlations between variables in the steady and unstable states under this flow situation [28, 29].

This research was prepared as a preliminary laboratory study to achieve a moving hydraulic jump with controlled discharges. It is an initial part of the study that is being prepared to treat the salt tide occurring in the Shatt al-Arab due to the lack of water imports that were coming from the Karun and Karkheh rivers from Iranian territory, as this scarcity caused a salt tide that affected significantly the environmental reality of the city of Basra and the agricultural lands surrounding the Shatt al-Arab, such as the Shatt al-Arab district and the Siba orchards. As part of the proposed solutions, a moving hydraulic jump is created that pushes the salt tongue into the Persian Gulf; the results were promising.

2. Experimental Works

The trapezoidal flume utilized in the experiment was 10 meters long, 0.25 meters wide, and 0.45 meters deep. Its sidewall slope (1:1) was made of clear glass, while its manometers were installed along the centerline of the steel-framed depression. A revolving flap tailgate was built at the flume's downstream end to regulate the flow depth. Water was delivered to the flume entrance through a pipe with a control valve from a sizable constant-head reservoir. Water entered an underground reservoir from the flume's downstream end and was pumped back up to the reservoir with a stable head. Figure 2 shows the flume profile and top view. A rectangular spillway was constructed within the flow circulation path and utilized for flow adjustment. A sluice gate was constructed to create the necessary conditions for generating a moving hydraulic leap at the flume's downstream side, 0.8 meters from the entrance. A low-head pressure transducer attached to a data-gathering tool was used to measure the water surface altitude at the upstream side of the sluice gate. Figure 3 shows the lab hydraulic jump, and Figure 4 is the schematic diagram.

Figure 2. Flume channel in hydraulic laboratory

Figure 3. Hydraulic Jump in flume channel

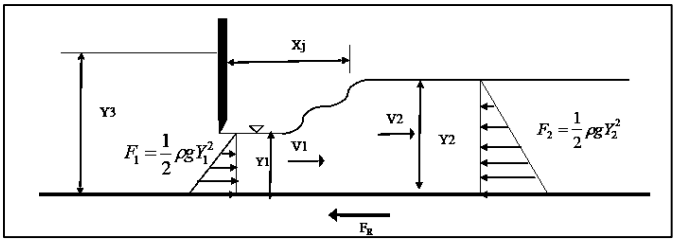

Figure 4. The schematic diagram of the hydraulic jump

The transducer was attached to a manometer tube placed safely away from the flume and calibrated there before usage to obliterate the transducer records' vibrational effects. A typical magnitude of 0.65 was employed for the gate's contraction coefficient throughout the initial stage of the experiment, which involved calibrating the sluice gate. The needed factors, such as the water surface profile and flow depth with time, were identified after the moving hydraulic jump was recorded. The sluice gate's calibration allowed for easier recording of the flow hydrographs produced on its upstream side. The gateway width was chosen so that, depending on the minimum flow rate, a hydraulic leap was produced close to the gate. As a result, during the rising phase of the hydrographs, there would be sufficient length in the downstream direction to support the moving hydraulic leap. The upstream supply pipe's control valve was moved continuously and gradually during each run to create the flow hydrograph. Each hydrograph was created by progressively opening the valve to its maximum setting. Throughout this stage, the leap descended, and throughout the hydrograph's falling phase, it turned around and headed for the sluice gate upstream. The experimental setup allowed for the comprehensive recording of the unsteady flow data.

3. Theoretical Analysis

In every operation, the whole data gathered has been documented. The information for the moments when the flow factors seemed to alter in magnitude owing to fluctuations in the boundary circumstances was considered and collated for future analysis. Depending on the well-known steady-state Bélanger formula, additionally, the unsteady supercritical flow depth, y_{1U}, also linked with the stable equivalent depth, y_{2S}, was calculated and tabulated. These unstable flow features comprised flow at the gate location, Q_g, and all flow depths that were tabulated for specific times instantly downstream and upstream of the jump front, y_{2U} and y_{1U}. In this context, it was thought that the variation between y_{2S} and y_{2U} influenced the properties of the moving leap. A thorough data analysis revealed no changes to the discharge along each run from the entrance opening to the spot where the leap was in motion. Therefore, the fluctuation that occurs in each reach was regarded as zero and disregarded.

As was previously mentioned, the y_{2S} was evaluated utilizing the Bélanger formula:

$$y_{2s} = 0.5\, y_1\{(1+8F_r^2)^{0.5} -1\} \quad (2)$$

Once the total energy at section 2 can be calculated using measured flow factors and steady-state flow factors, respectively, by using Equations 3 and 4, where the pressure distribution at section 2 is assumed to be hydrostatic and the discharge variation along the relatively short distance between sections 1 and 2 are ignored:

$$H_{2u} = Z_2 + \{Q_g^2/2gy_{2u}^2\} + P_{2u}/\gamma = S_o\,\{L - X_{y2}\} + \{Qg2/2gy_{2u}^2\} + y_{2u} \quad (3)$$

$$H_{2S} = Z_2 + \{Q_g^2/2gy^2_{2S}\} + P_{2S}/\gamma = So\,\{L - X_{y2}\} + \{Qg2/2gy^2_{2S}\} + y_{2S} \quad (4)$$

which H_{2u} is energy is calculated utilizing the downstream side of the jump front's estimated unstable flow depth, H_{2S} is Total energy was calculated depending on the anticipated steady conjugate depth, Z is lowering altitude, S_o is the bed slope, L is channel length, and X_{y2} is the spacing between the sluice gate and the location of y_{2u}.

4. Results Discussion

This study presented and examined the information relevant to three distinct hydrographs. The curves taken at the sluice gate's upstream end of the experimental setup are shown in Figure 5. Each hydrograph has markers identifying the points, whereas the data was tallied and evaluated. As previously stated, the discharge along the supercritical stretch was considered constant and equal to Q_g, the flow upstream of the gate at any given time. But the discharge at the moving jump's downstream side, Q_u, differs from that at the upstream side, Q_g. Backwater effects, unsteady flow, and unknown momentum formula factors may influence the discharge magnitude. The imbalance of forces operating over the leap front could cause the discrepancy between H_{2u} and H_{2S}.

Figure 6 plots the given variance in total energy versus the mentioned variance in associated depths in both dimensional and dimensionless versions. Figures 4 and 5 show the following linear correlation, which is satisfactory:

$$H_{2u} - H_{2S} = 0.721\,(y_{2u} - y_{2S}) \quad (5)$$

As a result, it is possible to anticipate how the supercritical front's downstream side will discharge utilizing the available data and the linear connection shown in Figures 6 and 7. Substituting the total energy terms in Equation 5 produces:

$$(y_{2u} - y_{2S}) + [(V^2_{2u} - V^2_{2S})/2g] = 0.721\,(y_{2u} - y_{2S}) \quad (6)$$

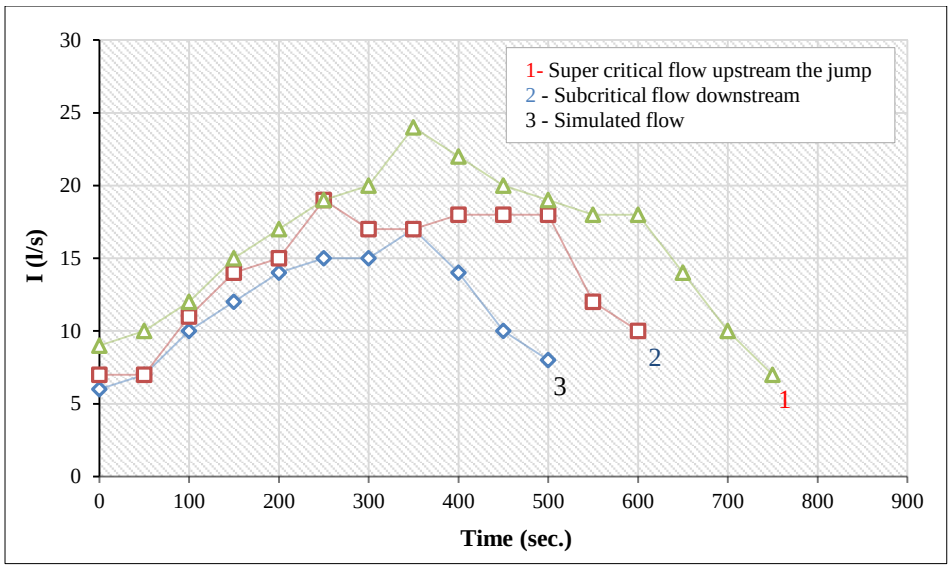

Figure 5. Recorded hydrograph

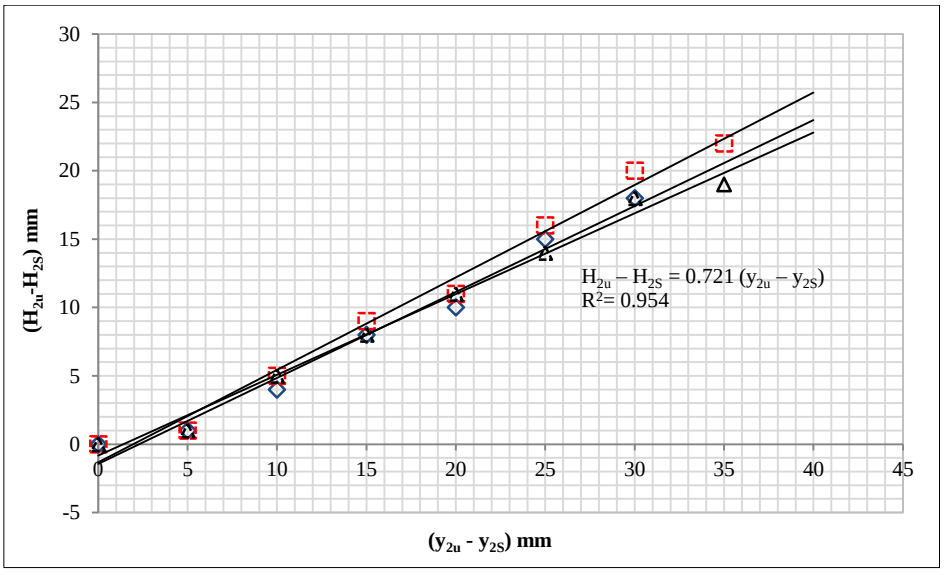

Figure 6. Correlation (a) between depth and energy disparities

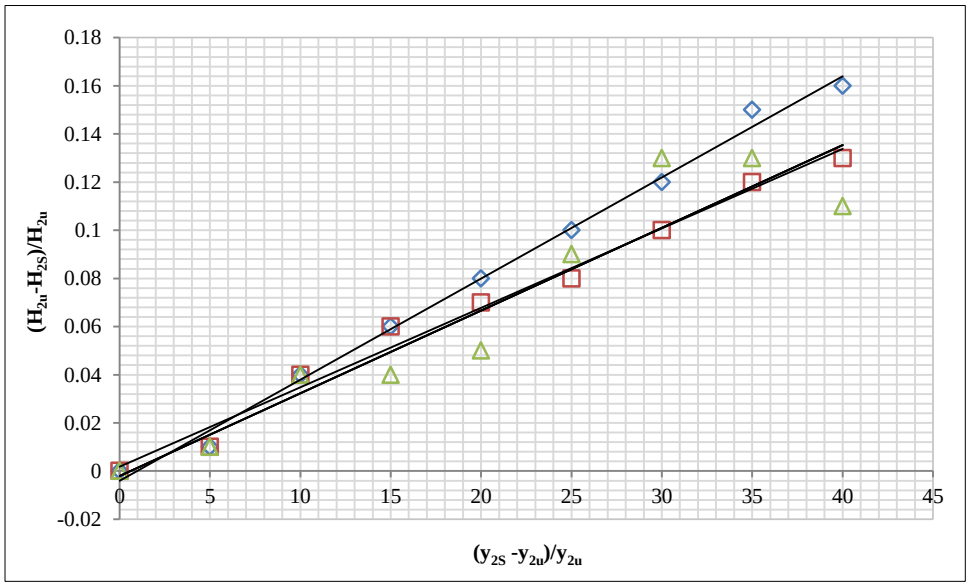

Figure 7. Variations in relative depth and in relative energy

In Equation 6, the velocities are replaced by the discharges and cross-section areas, and the result is:

$$6.22(y_{2u} - y_{2S}) = [(Q_u\, y_{2S} - Q_g\, y_{2u})/b(y_{2u} - y_{2S})]^2 \quad (7)$$

Q_u's solution to Equation 7 results in the following:

$$Q_u\, [\{(6.22\, b^2\, y^2_{2u}\, y^2_{2S}\, (y_{2u} - y_{2S}) + (Q_g\, y_{2u})^2\}/y_{2S}]^{0.5} \quad (8)$$

Since the magnitudes of Q_u were obtained from the data from the chosen intervals and included them, the proportion Q_u/Q_g could also be assessed in the spreadsheet. Plotting the magnitudes of $(y_{2u}\text{-}y_{2S})/y_{2u}$ or $(H_{2u}\text{-}H_{2S})/H_{2u}$ versus Q_u/Q_g indicates trustworthy correlations between the visual flow immediately downstream; Figures 8 and 9 show the jump front and the release discharged from the gate opening.

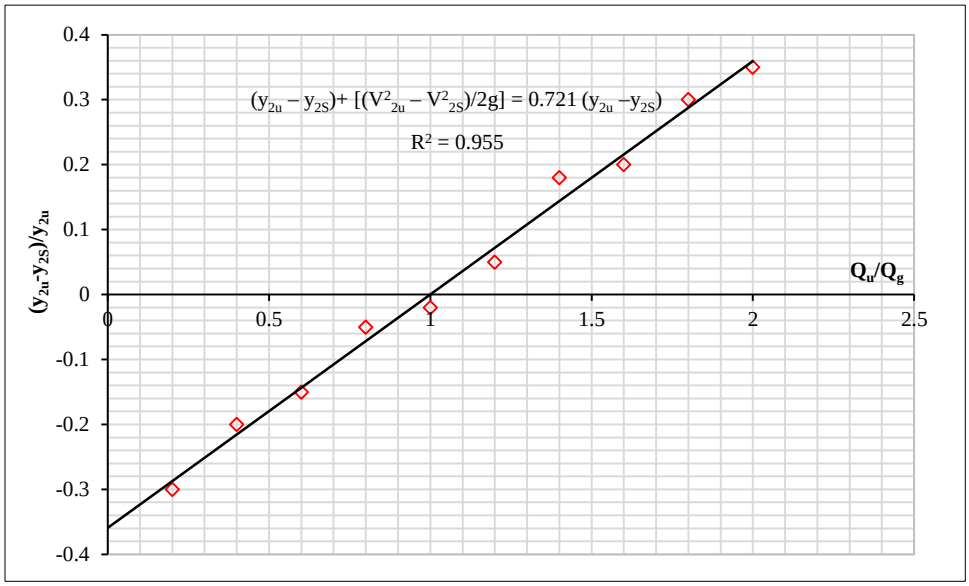

Figure 8. Correlation between relative subcritical flow depth fluctuations

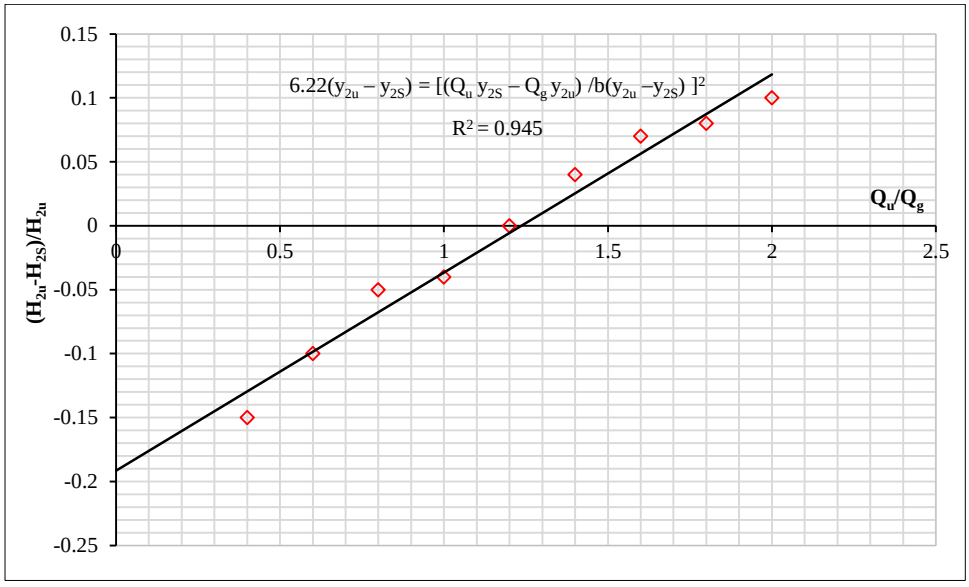

Figure 9. Correlation between discharge proportion and relative energy variation

With Q_U, the following formula represents the control volume's steady state momentum for both sides of the jump front:

$$\sum F_X - F_{P1} - F_{P2u} + W\sin\dot{\alpha} - F_F = \rho\, Q\, (V_{2u} - V_1) \quad (9)$$

In which ($W\sin\dot{\alpha}$) and F_F] are the friction force and the weight component in the flow direction, respectively; F_{P1} and

F_{P2U} are the forces operating on the relevant pieces. Due to the short length of the control volume and the slight longitudinal slope of the channel, the subsequent forces are zero and may be ignored without affecting the outcomes.

Thus, the formula that results is as follows:

$$F_{p1}- F_{P2u} = \rho(Q_u V_{2u} – Q_g V_1)= \rho\{(Q_u^2/by_{2u})-(Q_g^2/by_1)\} \quad (10)$$

Solving Equation 10 results in:

$$F_{p2u}/\rho=F(y_{2u})=(y_1^2 b/2)-(1/gb)\{(Q_u^2/y_{2u} – Q_s^2/y_1) \quad (11)$$

The magnitudes of F_{P2U}/γ are determined by assessing the right side of Equation 11 depending on magnitudes. Real energy force (which is different from the hydraulic force) positioned on the advancing leap front's downstream side, as indicated by F_{P2U}, should consider F_{p2u}^{th}. The classic hydraulic force term of trapezoidal cross areas [$\gamma y_{2S}^2 b/2$ and $\gamma y_{2u}^2 b/2$]. A study of moving hydraulic Jumps in trapezoidal channels can be utilized to calculate the hydraulic magnitudes, which Fbp2u denotes. Figure 10 shows the pressure force at the jump front's subcritical region. Each run's flow situation displayed distinct behavior that differed from that detected in other runs. Nevertheless, the results from all of these hydrographs match the pattern predicted by Equation 5. Although the longitudinal slope was the same for all runs, it appears that the result is supported by characteristics like latitudinal slope and border roughness, which only affect how steeply the line slopes in Equation 5.

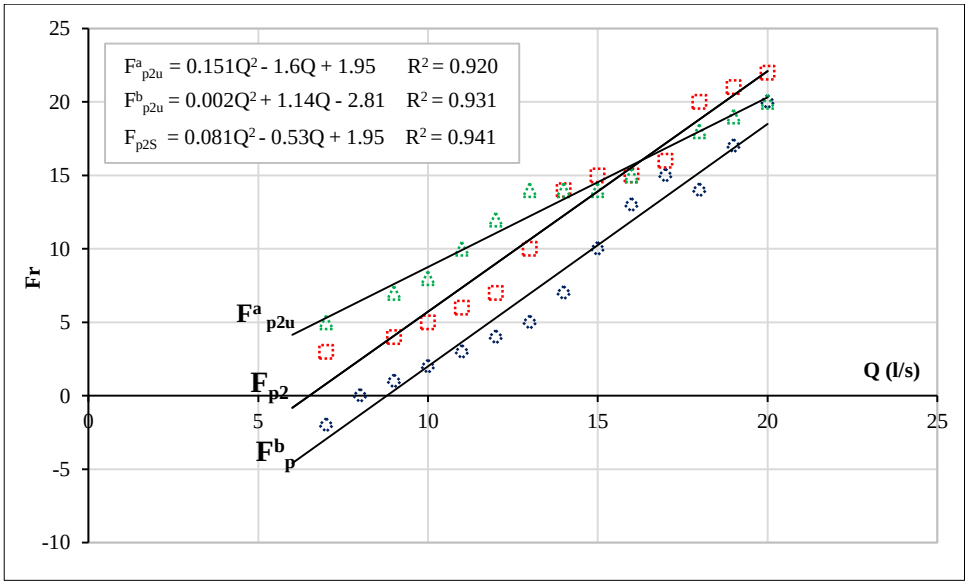

Figure 10. Immediately behind the supercritical flow front, pressure force

When utilizing Equations 3 and 4 to calculate the total energy, two fundamental assumptions were taken into account:

- Hydrostatic pressure distributions were detected across the jump fronts.
- The identical discharge magnitudes can be seen on both sides of the jump front.

According to Figure 8, the pressure distribution in the subcritical area is bigger for small discharges and lower for large discharges than for the hydrostatic magnitude. Equation 11 is used to compute the pressure force in the subcritical region, and this method shows that y2S estimates the hydrostatic pressure force, which is always less than this force. However, when the discharge increases, the variance decreases.

Several experiments were carried out in an open channel in a laboratory to determine the correlation between moving hydraulic jump characteristics. The flume bed friction was considered for correlating the stationary and moving hydraulic jump parameters in a non-dimensional form.

5. Conclusion

At the upstream end of the flume, three different-shaped hydrographs were generated; each hydrograph's unstable flow features were continuously logged. Data from particular discharges in each hydrograph were linked to stable factors linked to the discharges and their supercritical flow characteristics. The comparison indicates that the stable and unstable components are consistently correlated. The assessment of unstable merged flow conditions referring to stable condition

correlations feels trustworthy and useful, despite several simplifying assumptions being used to drive such correlations. However, more information and data were needed before drawing any generalizations, especially for different border roughness and longitudinal slopes.

Several experiments were carried out in an open channel in a laboratory to determine the correlation between moving hydraulic jump characteristics. The flume bed friction was considered for correlating the stationary and moving hydraulic jump parameters in a non-dimensional form. It is advised to do additional research and tests using various discharges to confirm this study's findings. Comprehensive research also requires tests with various border roughness and channel slopes. It was not reliant on the gate opening size and whether there were any linear correlations between the jump characteristics. Relationships that depended on the size of the gate opening were sometimes non-linear. The flow rate has a linear relationship with bed friction. Over the leap front, a pressure difference rises from hydrostatic pressure at the gate to a value higher than that downstream. For a moving hydraulic jump, it was found that the pressure force downstream is affected by the flow rate at the gate, the downstream flow rate, bed friction, supercritical depth, and sub-critical depth. An empirical formula for the flow rate downstream for moving hydraulic jumps was established using theoretic formulas and experimental findings.

6. Declarations

6.1. Author Contributions

Conceptualization, N.A., S.H., and M.K.; methodology, N.A., S.H., and M.K.; validation, M.K., F.A., and Z.A.; formal analysis, Z.A.; investigation, N.A., S.H., and M.K.; resources, Z.A.; data curation, F.A.; writing—original draft preparation, N.A., S.H., Z.A., F.A., and M.K.; writing—review and editing, M.K. and S.H.; visualization, Z.A.; supervision, N.A. All authors have read and agreed to the published version of the manuscript.

6.2. Data Availability Statement

The data presented in this study are available in the article.

6.3. Funding

The authors received no financial support for the research, authorship, and/or publication of this article.

6.4. Conflicts of Interest

The authors declare no conflict of interest.

7. References

[1] Sun, B., Zhu, S., Yang, L., Liu, Q., Zhang, C., & Zhang, J. ping. (2021). Experimental and Numerical Investigation of Flow Measurement Mechanism and Hydraulic Performance on Curved Flume in Rectangular Channel. Arabian Journal for Science and Engineering, 46(5), 4409–4420. doi:10.1007/s13369-020-04949-x.

[2] Xiao, Y., Wang, W., Hu, X., & Zhou, Y. (2016). Experimental and numerical research on portable short-throat flume in the field. Flow Measurement and Instrumentation, 47, 54–61. doi:10.1016/j.flowmeasinst.2015.11.003.

[3] Sun, B., Yang, L., Zhu, S., Liu, Q., Wang, C., & Zhang, C. (2021). Study on the applicability of four flumes in small rectangular channels. Flow Measurement and Instrumentation, 80, 101967. doi:10.1016/j.flowmeasinst.2021.101967.

[4] Ran, D., Wang, W., & Hu, X. (2018). Three-dimensional numerical simulation of flow in trapezoidal cutthroat flumes based on FLOW-3D. Frontiers of Agricultural Science and Engineering, 5(2), 168–176. doi:10.15302/J-FASE-2018217.

[5] Savage, B., Heiner, B., & Barfuss, S. L. (2013). Parshall Flume Discharge Correction Coefficients Through. Journal of Water Management. 167(5), 279-287. doi:10.1680/wama.12.00112.

[6] Willeitner, R. P., Barfuss, S. L., & Johnson, M. C. (2013). Using Numerical Modeling to Correct Flow Rates for Submerged Montana Flumes. Journal of Irrigation and Drainage Engineering, 139(7), 586–592. doi:10.1061/(asce)ir.1943-4774.0000576.

[7] Watral, Z., Jakubowski, J., & Michalski, A. (2015). Electromagnetic flow meters for open channels: Current state and development prospects. Flow Measurement and Instrumentation, 42, 16–25. doi:10.1016/j.flowmeasinst.2015.01.003.

[8] Savage, B. M., Heiner, B., & Barfuss, S. L. (2014, May). Parshall flume discharge correction coefficients through modelling. Proceedings of the Institution of Civil Engineers, Water Management, 167(5), 279-287. doi:10.1680/wama.12.00112.

[9] Heyrani, M. (2022). Numerical Modeling of Flow in Parshall Flume Using Various Turbulence Models. Ph.D. Thesis, University of Ottawa, Ottawa, Canada.

[10] Panchigar, D., Kar, K., Shukla, S., Mathew, R. M., Chadha, U., & Selvaraj, S. K. (2022). Machine learning-based CFD simulations: a review, models, open threats, and future tactics. Neural Computing and Applications, 34(24), 21677–21700. doi:10.1007/s00521-022-07838-6.

[11] Katopodes, N. D. (2018). Free-surface flow: environmental fluid mechanics. Butterworth-Heinemann, Oxford, United Kingdom.

[12] Tu, J., Yeoh, G. H., & Liu, C. (2018). Computational fluid dynamics: a practical approach. Butterworth-Heinemann, Oxford, United Kingdom.

[13] Clemmens, A. J., Wahl, T. L., Bos, M. G., & Replogle, J. A. (2001). Water measurement with flumes and weirs (No. 58). International Institute for Land Reclamation and Improvement/ILRI, Washington, United States.

[14] Heyrani, M., Mohammadian, A., & Nistor, I. (2021). Numerical simulation of flow in Parshall flume using selected nonlinear turbulence models. Hydrology, 8(4), 151. doi:10.3390/hydrology8040151.

[15] Heyrani, M., Mohammadian, A., Nistor, I., & Dursun, O. F. (2021). Numerical modeling of Venturi flume. Hydrology, 8(1), 1–17. doi:10.3390/hydrology8010027.

[16] Imanian, H., & Mohammadian, A. (2019). Numerical simulation of flow over ogee crested spillways under high hydraulic head ratio. Engineering Applications of Computational Fluid Mechanics, 13(1), 983–1000. doi:10.1080/19942060.2019.1661014.

[17] Khosronejad, A., Herb, W., Sotiropoulos, F., Kang, S., & Yang, X. (2021). Assessment of Parshall flumes for discharge measurement of open-channel flows: A comparative numerical and field case study. Measurement, 167, 108292. doi:10.1016/j.measurement.2020.108292.

[18] Dursun, O. F. (2016). An experimental investigation of the aeration performance of parshall flume and venturi flumes. KSCE Journal of Civil Engineering, 20(2), 943–950. doi:10.1007/s12205-015-0645-0.

[19] Bijankhan, M., & Kouchakzadeh, S. (2015). The hydraulics of parallel sluice gates under low flow delivery condition. Flow Measurement and Instrumentation, 41, 140–148. doi:10.1016/j.flowmeasinst.2014.10.017.

[20] Rezaie Shaddehi, F., & Bijankhan, M. (2020). Experimental study on free and submerged multi-jets. Flow Measurement and Instrumentation, 75, 101805. doi:10.1016/j.flowmeasinst.2020.101805.

[21] Sauida, M. F. (2013). Reverse flow downstream multi-vent regulators. Ain Shams Engineering Journal, 4(2), 207–214. doi:10.1016/j.asej.2012.09.002.

[22] Zerihun, Y. T. (2016). A numerical study on curvilinear free surface flows in Venturi flumes. Fluids, 1(3), 21. doi:10.3390/fluids1030021.

[23] Tiwari, N. K., & Sihag, P. (2020). Prediction of oxygen transfer at modified Parshall flumes using regression models. ISH Journal of Hydraulic Engineering, 26(2), 209–220. doi:10.1080/09715010.2018.1473058.

[24] Tekade, S. A., Vasudeo, A. D., Ghare, A. D., & Ingle, R. N. (2016). Measurement of flow in supercritical flow regime using cutthroat flumes. Sadhana, 41(2), 265–272. doi:10.1007/s12046-016-0463-1.

[25] Robertson, E. D., Chitta, V., Walters, D. K., & Bhushan, S. (2014). On the Vortex Breakdown Phenomenon in High Angle of Attack Flows over Delta Wing Geometries. Volume 1: Advances in Aerospace Technology. doi:10.1115/imece2014-39354.

[26] Ribeiro, Á. S., Alves e Sousa, J., Simões, C., Lages Martins, L., Dias, L., Mendes, R., & Martins, C. (2021). Parshall flumes flow rate uncertainty including contributions of the model parameters and correlation effects. Measurement: Sensors, 18, 100108. doi:10.1016/j.measen.2021.100108.

[27] Qian, S. Tuo, Zhang, Y., Xu, H., Wang, X. Sheng, Feng, J. Gang, & Li, Z. Xiang. (2021). Effects of surface roughness on overflow discharge of embankment weirs. Journal of Hydrodynamics, 33(4), 773–781. doi:10.1007/s42241-021-0068-y.

[28] Adedoyin, A. A., Walters, D. K., & Bhushan, S. (2015). Investigation of turbulence model and numerical scheme combinations for practical finite-volume large eddy simulations. Engineering Applications of Computational Fluid Mechanics, 9(1), 324–342. doi:10.1080/19942060.2015.1028151.

[29] Li, P., Zhu, D. Z., Xu, T., & Zhang, J. (2022). Air Demand of a Hydraulic Jump in a Closed Conduit. Journal of Hydraulic Engineering, 148(2). doi:10.1061/(asce)hy.1943-7900.0001963.